

# Qubit Motion as a Microscopic Model for the Dynamical Casimir Effect

A. Agustí,<sup>1</sup> L. García-Álvarez,<sup>2</sup> E. Solano,<sup>3, 4, 5, 6</sup> and C. Sabín<sup>1</sup>

<sup>1</sup>*Instituto de Física Fundamental, CSIC, Serrano 113-bis 28006 Madrid, Spain*

<sup>2</sup>*Department of Microtechnology and Nanoscience (MC2),*

*Chalmers University of Technology, SE-412 96 Göteborg, Sweden*

<sup>3</sup>*International Center of Quantum Artificial Intelligence for Science and Technology (QuArtist)*

*and Physics Department, Shanghai University, 200444 Shanghai, China*

<sup>4</sup>*Department of Physical Chemistry, University of the Basque Country UPV/EHU, Apartado 644, 48080 Bilbao, Spain*

<sup>5</sup>*IKERBASQUE, Basque Foundation for Science, María Diaz de Haro 3, 48013 Bilbao, Spain*

<sup>6</sup>*IQM, Nymphenburgerstr. 86, 80636 Munich, Germany*

The generation of photons from the vacuum by means of the movement of a mirror is known as the dynamical Casimir effect (DCE). In general, this phenomenon is effectively described by a field with time-dependent boundary conditions. Alternatively, we consider a microscopic model of the DCE capable of reproducing the effect with no time-dependent boundary conditions. Besides the field, such a model comprises a new subsystem modeling the mirror's internal structure. In this work, we study the most straightforward system for the mirror: a qubit moving in a cavity and coupled to one of the bosonic modes. We find that under certain conditions on the qubit's movement that do not depend on its physical properties, a large number of photons may be generated without changing the qubit state, as should be expected for a microscopic model of the mirror.

In his seminal paper of 1970, G. Moore [1] discovered that relativistic movement of perfectly conducting mirrors could produce radiation even if the state of the electromagnetic field before the mirrors' movement were the vacuum. In the next years, the phenomenon was subsequently studied [2–4] until the name *Dynamical Casimir Effect* (DCE) was coined [5], joining the broad family of quantum vacuum fluctuation effects among which we find nowadays the Lamb shift [6], the *static* Casimir effect [7, 8] and the Unruh [9–11] and Hawking's radiations [12], to name a few. For a long time, the realization of DCE and most of these effects remained out of reach due to the experimental requirements to access the quantum and relativistic parameter regime needed for a measurable signal. This changed with the advent of circuit quantum electrodynamics this century, which made possible experiments in the strong light-matter coupling regime [13] as well as to modulate the magnitude of that coupling over time. In 2011, C.M. Wilson *et al* [14] carried out an experiment in which the relativistically moving mirror was reproduced using a modulated magnetic flux threading a superconducting quantum interference device, leading to a time-dependent boundary condition in a microwave waveguide and to a measurable DCE photon production. The DCE was also observed in a Josephson metamaterial capable of modulating its refractive index [15], leading to an equivalent setting in which the effective length of a cavity changes over time.

In this new scenario where the DCE is combined with the comprehensive toolset of present-day quantum technologies, open questions may now be accessible to experiments. In this work, we address the analysis of a microscopic model for the mirrors, in contrast with previous descriptions of the effect with time-dependent boundary conditions. That is, we consider a model in which the DCE takes place due to the interaction of the field with a new system described by its own degrees of freedom.

This new system represents the internal degrees of freedom of the mirror, and thus we will refer to it as a *discrete mirror*. Such a system would be analogous, for example, to the particles forming a rigid body that fix the ends of a string. Regardless of their internal properties, as long as the state of these particles remains unchanged, the dynamics of the string will be governed by a differential equation with a fixed boundary. It becomes natural now to impose the same requirements to the discrete mirror: its state must not change and its internal parameters must be irrelevant for the production of the effect.

The problem of finding such a system has been tackled before in the ideal setting of a non-relativistic oscillating atom in free space [16]. However, such system does not fulfil all the requirements for a microscopic model and its experimental feasibility is difficult to assess. This is the gap this Letter bridges, and so we study the most straightforward system that may accommodate this phenomenon: a discrete mirror made of a qubit moving in a cavity and interacting with one of its bosonic modes. A diagram of the system can be found in Figure 1. This system has been studied extensively in the literature, especially in the case of a static qubit, in which it is better known as the Rabi model [17, 18] or, if the coupling is weak enough to adopt the rotating wave approximation (RWA), the Jaynes-Cummings (JC) model [19]. Even in the case with a moving qubit, prior work [20] has studied photon and qubit excitation due to the so-called cavity-enhanced Unruh effect [21–24]. However, the parameter regime found to reproduce the DCE, that is, to produce radiation without changing the internal state of the discrete mirror, has not been explored before, to the authors' knowledge. In this Letter we show that qubit motion at the mode's frequency generates photons without qubit excitation, providing a microscopic model for the DCE.

The structure of this Letter is as follows: Firstly, we

will introduce the system's Hamiltonian and discuss some of its features and approximations. Secondly, we will present a numerical exploration of the system's parameter space, finding both the JC model and the cavity-Unruh regime, as well as the novel *microscopic* DCE regime. Then we will present a perturbative justification for the *microscopic* DCE regime, which will lead to a better characterization of the phenomenon as a second-order perturbation theory effect.

The discrete mirror is considered a point-like electric dipole qubit coupled to one bosonic field mode, thus it is described by the Hamiltonian

$$\begin{aligned} H_{\text{total}} &= H_0 + H_{\text{int}} \\ H_0 &= \Omega S_z + \omega a^\dagger a \\ H_{\text{int}} &= g(t) \sigma_x (a^\dagger + a), \end{aligned} \quad (1)$$

where  $\Omega$  and  $\omega$  are the qubit and mode frequencies,  $S_z$  is the spin operator on the  $z$  axis,  $\sigma_x$  the first Pauli matrix,  $a^\dagger$  and  $a$  the creation and annihilation operators for the bosonic mode and  $g$  the coupling, which is time dependent due to the classical motion of the discrete mirror qubit. If the bosonic mode is the fundamental mode of a cavity with perfectly conducting and static edges, then the coupling is of the form

$$\begin{aligned} g(t) &= g_0 \cos(kx(t)) \\ k &= \pi/L, \end{aligned} \quad (2)$$

where  $L$  is the length of the cavity and  $x$  the trajectory of the discrete mirror qubit. The coupling intensity,  $g_0$ , is very low in any realistic setting, not to mention the difficulty of driving an atom's movement to relativistic speeds. Thus, the typical approach to experiment design is to create an analog system and simulate the effect there. For example, this Hamiltonian can be engineered in the setting of circuit quantum electrodynamics using tunable-coupling qubits, for which several proposals have been made [25]. Alternatively, a promising candidate consists of using film bulk acoustic resonators, which could perform the role of an actual moving discrete mirror [26, 27].

Given the linearity of the Schrödinger equation, we expect a coupling modulated with a cosine shape with a well-defined frequency to be the most appropriate for analytical calculations. Such cosine coupling is produced by trajectories with constant velocity  $x = vt$ . In that case the coupling would oscillate with a driving frequency  $\omega_d = \pi v/L$ . However, such trajectories are not bounded to the cavity. Despite this fact, a pure cosine coupling is possible if the (otherwise constant) velocity of the qubit is inverted every time it reaches the edges of the cavity, and this is the trajectory we analyze.

Figures 2 and 3 show the number of photons and the expectation value of  $S_z$  as a function of time and qubit velocity when the system evolves from its ground state under the Hamiltonian of Eq. (1), for the resonant case with  $\omega = \Omega$  and the trajectory mentioned above. When

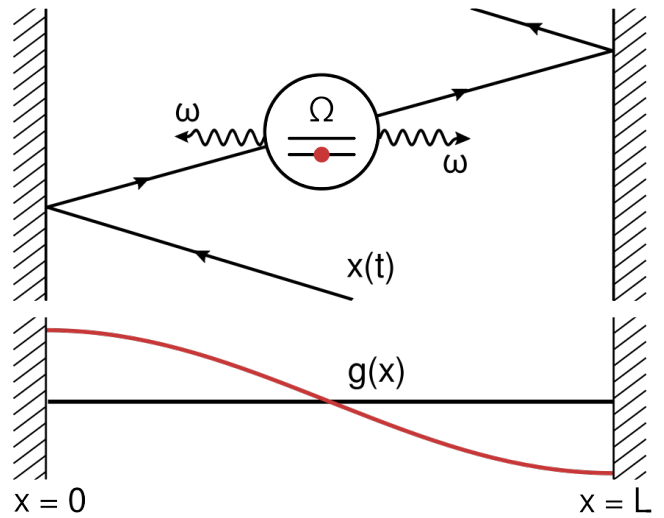


FIG. 1. (Upper panel) Diagram of the system. The generation of photons from vacuum is not produced by time-dependent boundary conditions, the walls (dashed dark blocks) are static. Instead, the dynamical Casimir effect takes place due to a qubit (circle containing two segments, representing two levels with energy gap  $\Omega$ ) moving back and forth in the cavity with constant speed  $|v| = \pi L/\omega$ , where  $\omega$  is the frequency of the fundamental mode photons and  $L$  the length of the cavity. The qubit behaves as a *discrete mirror* in the sense of producing photons without changing its state and regardless of its internal frequency  $\Omega$ . (Lower panel) Qubit-mode coupling  $g$  as a function of qubit position for the fundamental mode, as defined in Eqs. (1) and (2). Then, the time dependent coupling is due to its composition with the trajectory and a small abuse in notation  $g(t) = g(x(t))$ .

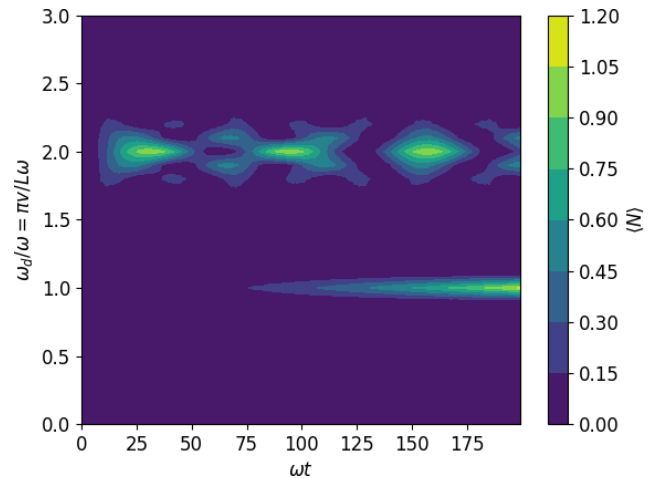


FIG. 2. Number of photons  $\langle N \rangle$  as a function of time  $t$  in units of the mode frequency  $\omega$ , and driving frequency  $\omega_d$  in units of the same mode frequency  $\omega$ . The driving frequency was produced by a qubit moving back and forth within the cavity, with constant velocity  $v = L/\pi\omega_d$  in one direction, and  $-v$  after bouncing in the opposite direction. The qubit frequency is given by  $\Omega = \omega$ , and the coupling intensity is  $g_0 = 0.1\omega$ .

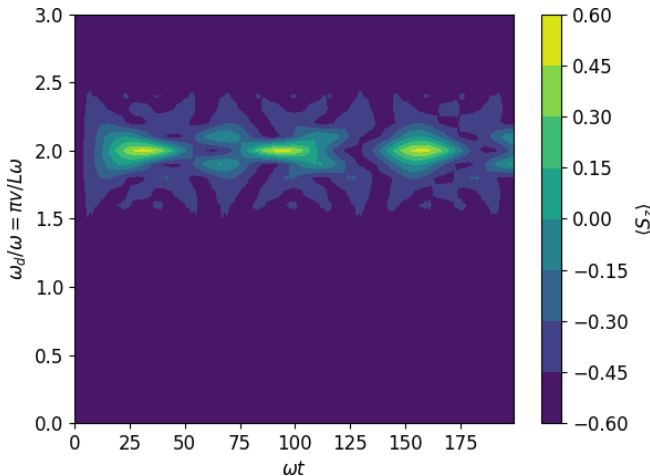


FIG. 3. Expectation value  $\langle S_z \rangle$  as a function of time  $t$  in units of the mode frequency  $\omega$ , and driving frequency  $\omega_d$  in units of the same mode frequency  $\omega$  in the same conditions than Figure 2.

the velocity is zero, the coupling is constant, and given the relatively low coupling intensity  $g_0 = 0.1\omega$ , the rotating wave approximation (RWA) and the JC model hold, that is, the counter-rotating terms  $a^\dagger\sigma^+$  and  $a\sigma^-$  produce no dynamics given their fast phase in the interaction picture. Moreover, given that the initial state is the ground state, the rotating terms  $a^\dagger\sigma^-$  and  $a\sigma^+$  that compose the JC model produce no dynamics either.

When the driving frequency is twice the qubit or bosonic mode frequencies  $\omega_d = 2\omega = \omega + \Omega$ , or in terms of the qubit velocity  $v = 2\omega L/\pi$ , the *anti*-RWA holds, neglecting the now fast-oscillating rotating terms, leaving the now constant counter-rotating ones and producing the cavity-enhanced Unruh effect. In this scenario, the ground state is expected to evolve towards the state with the qubit excited and one photon, in a sort of Rabi oscillation, as we observe in the numerical exploration for the appropriate qubit velocity. However, Figure 2 shows another feature. When all the frequencies of the system (qubit frequency  $\Omega$ , mode frequency  $\omega$  and driving  $\omega_d$ ) are resonant, a non-oscillatory monotonic photon production without qubit dynamics is observed. This photon generation is the proposed *microscopic* Dynamic Casimir effect. If the system is evolved further in time, the ever increasing number of photons requires a bigger subspace of the Hilbert space to be considered in the simulations. See Appendix A for proof that said subspace was large enough.

A perturbative approach can be successful to understand why the *microscopic* DCE takes place, very much as it happens with the RWA or the Unruh effect. We will not pay much attention to the RWA since the initial state we consider, the ground state, does not evolve in time under this approximation. Thus, we focus our attention now to the cavity-enhanced Unruh effect, in

which the Hamiltonian, in the Schrödinger picture

$$H_{\text{anti-RWA}} = e^{-i(\omega+\Omega)t} a^\dagger \sigma^+ + e^{i(\omega+\Omega)t} a \sigma^- \quad (3)$$

produces the same resonant perturbative corrections than the full Hamiltonian in Eq. (1). Thus, it becomes a good approximation to consider the new Hamiltonian instead of the complete one. However, in the *microscopic* DCE it is not straightforward to find a simple Hamiltonian that reproduces all the same resonances the Hamiltonian in Eq. (1) would produce under the appropriate qubit velocity, since both rotating and counter-rotating terms oscillate with similar frequency, and thus neither of them can be neglected. Nevertheless, the resonances are still a great tool capable of predicting properties of this radiation, only this time they are produced at second order and every other even order. To clarify this, let us fix some notation. A perturbative expansion of the state in terms of the coupling intensity  $g_0$  is

$$\psi(t; g_0) = \psi^{(0)} + \psi^{(1)}(t)g_0 + \frac{1}{2}\psi^{(2)}(t)g_0^2 + \dots \quad (4)$$

Each of the terms  $\psi^{(n)}(t)$  is a partial derivative of the state with respect to  $g_0$  and evaluated in  $g_0 = 0$

$$\psi^{(n)}(t) = \partial_{g_0}^n \psi(t; g_0 = 0).$$

Despite the functional dependence of  $\psi(t; g_0)$  is hardly ever known, time-dependent perturbation theory is useful because, firstly,  $\psi^{(0)}$  is just the initial state and, secondly, each correction can be computed from the previous one

$$\psi^{(n+1)}(t) = \int_0^t dt' \frac{H(t')}{g_0} \psi^{(n)}(t') \quad (5)$$

where  $H$  is the interaction Hamiltonian  $H_{\text{int}}$  in the interaction picture with respect to the static  $H_0$ . Now it is straightforward to write

$$\begin{aligned} \psi^{(2)}(t) &= \int_0^t dt' \int_0^{t'} dt'' \frac{H(t')}{g_0} \frac{H(t'')}{g_0} |g, 0\rangle = \\ &\int_0^t dt' \int_0^{t'} dt'' e^{-i\omega t'} \sigma^- a^\dagger e^{-i\omega t''} e^{i2\omega t''} \sigma^+ a^\dagger |g, 0\rangle + O(t^0), \end{aligned} \quad (6)$$

where  $|g\rangle$  is the ground state vector for the qubit and  $|n\rangle$  is the  $n$ -photon state in the bosonic mode. With  $O(t^0)$ , we indicate that we neglect any term bounded by a constant for long enough times, in this case constants and exponentials with imaginary argument. The  $e^{-i\omega t}$  terms are due to the coupling driving and the  $e^{i2\omega t}$  one is due to the interaction picture time dependence of the counter-rotating term  $\sigma^+ a^\dagger$ . If the integration is carried out the result is

$$\langle g, 2 | \psi^{(2)}(t) \rangle = \frac{g_0^2 \sqrt{2}it}{4\omega} + O(t^0). \quad (7)$$

Notice how a *resonance* has taken place, in the sense of having a contribution to the  $|g, 2\rangle$  component linear in

time  $t$ , and not just some imaginary exponential. It is worth noting too, that the resonance increases the contribution to the state of the vector  $|g, 2\rangle$  and not other vectors, a compatible result with Figures 2 and 3 where there were photon production and no qubit excitation. New resonances happen for every higher even order in the components  $\langle g, 2n | \psi^{(2n)} \rangle$ , and the odd orders have no new resonances (see Appendix B). These formulae illustrate why there is an ever increasing photon production without appreciable qubit excitation. In addition to this, if the qubit, bosonic mode and driving frequencies are no longer resonant one gets

$$\psi^{(2)}(t) = \int_0^t dt' \int_0^{t'} dt'' \times e^{-i\omega_d t'} e^{i(\omega-\Omega)t'} \sigma^- a^\dagger e^{-i\omega_d t''} e^{i(\omega+\Omega)t''} \sigma^+ a^\dagger |g, 0\rangle. \quad (8)$$

If the frequency of the qubit is rewritten in terms of the mode frequency and some detuning  $\delta$ , so that  $\Omega = \omega + \delta$ , then

$$\psi^{(2)}(t) = \int_0^t dt' \int_0^{t'} dt'' \times e^{-i\omega_d t'} e^{-i\delta t'} \sigma^- a^\dagger e^{-i\omega_d t''} e^{i(2\omega+\delta)t''} \sigma^+ a^\dagger |g, 0\rangle, \quad (9)$$

from which one can deduce that the detuning compensates itself from the first order to the second order and that it is irrelevant in the photon production. The parameter relation that is critical in the *microscopic* DCE is that the driving frequency matches the mode frequency  $\omega_d = \omega$ .

This can be seen in Figure 4, which represents the maximum number of photons over the time interval  $t \in [0, 200/\omega]$  for different values of the qubit frequency  $\Omega$  and driving  $\omega_d$  for a fixed mode frequency  $\omega$  with a coupling intensity of  $g_0 = 0.1\omega$ . Note that regardless of the qubit frequency, photons are generated whenever the qubit's velocity is such that  $\omega_d = \omega$ , as expected. Even more so, increasing the qubit frequency reduces the photon generation due to its presence in the denominator of the perturbative corrections. The analog Unruh effect shows up again in this setting, consisting of that diagonal line in the region where  $\omega_d - \Omega = \omega$ . Notice how the photon number never exceeds one, as in a Rabi oscillation. Again, see Appendix A for tests on the accuracy of the simulations.

Regarding the experimental implementation, we remark that it does not require any additional sophistication with respect to the measurement of acceleration radiation or cavity-enhanced Unruh effect, either by means of a modulation of the coupling to mimic the qubit motion [20] or by actual mechanical oscillation [26, 28]. Indeed, while the Unruh effect appears for a qubit coupling modulation with frequency equal to the sum of the mode and qubit frequencies  $\omega_d = \omega + \Omega$ , the microscopic DCE appears at just the frequency of the mode  $\omega_d = \omega$ . Therefore, both effects should be observable in the same experimental setup. See Appendix C for further discussions on realistic experimental parameters and dissipation.

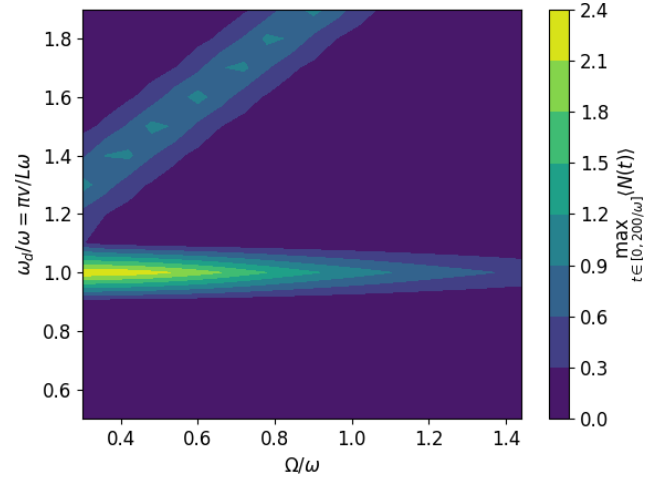


FIG. 4. Maximum number of photons  $\langle N \rangle$  in the time period  $t \in [0, 200/\omega]$ , that is  $\max_{t \in [0, 200/\omega]} \langle N(t) \rangle$ , for different values of the qubit's frequency  $\Omega$  in units of the mode's frequency  $\omega$  and different driving frequencies  $\omega_d$  in units of the mode frequency  $\omega$  too. Notice how the *microscopic* DCE regime does not depend on the qubit frequency, only on its velocity which, in turn, produces the driving. On the other hand, whenever  $\omega_d - \Omega = \omega$  the Unruh effect takes place and one photon and qubit excitation are produced as in a Rabi oscillation.

Summarizing, we have found that a discrete mirror composed of a qubit moving classically is capable of reproducing some of the features of the Dynamical Casimir Effect, such as photon generation from vacuum. The generation takes place regardless of the qubit's internal structure or state, which supports the hypothesis that the qubit is indeed behaving as a microscopic model for a moving mirror. This new effect is different from the already known cavity-enhanced Unruh effect, where the excitation of the qubit always accompanies the photon production. The *microscopic* DCE explored here also differs from a more idealized proposal consisting of an atom oscillating in free space [16]. In that case the frequency of the motion must match the sum of the frequencies of two modes which, in turn, must be very small compared to the atom's internal frequency. If we translate those requirements into our system, we find the scenario of a largely detuned qubit moving at twice the frequency mode, a different regime than the one found to produce the DCE. Finally, our proposal for the observation of both the cavity-enhanced Unruh effect and the microscopic DCE can be achieved in the same experiment, realizable in promising setups, such as superconducting circuits or mechanical oscillators.

A.A. and C.S have received financial support through the Postdoctoral Junior Leader Fellowship Programme from la Caixa Banking Foundation (LCF/BQ/11640005). L.G.-Á. acknowledges funding from the Wallenberg Center for Quantum Technology (WACQT). E.S. acknowledges financial support from Spanish MCIU/AEI/FEDER (PGC2018-095113-B-I00), Basque Government IT986-16, projects QMiCS (820505)

and Open-SuperQ (820363) of EU Flagship on Quantum Technologies, EU FET Open Grant Quromorphic, and Shanghai STCSM (Grant No. 2019SHZDZX01-ZX04).

### Appendix A: Numerical simulation details

We consider a system composed by a qubit of fixed frequency  $\Omega$  moving within a cavity of length  $L$  and coupled to its fundamental mode of frequency  $\omega$  and wavenumber  $k = \pi/L$ . Due to said movement, the coupling oscillates in time as  $g(t) = g_0 \cos(kx(t))$ , with  $x(t)$  the trajectory of the qubit. The system is described by the Hamiltonian of Eq. (1) that we rewrite here for convenience,

$$\begin{aligned} H_{\text{total}} &= H_0 + H_{\text{int}} \\ H_0 &= \Omega S_z + \omega a^\dagger a \\ H_{\text{int}} &= g(t) \sigma_x (a^\dagger + a). \end{aligned} \quad (\text{A1})$$

We simulate the dynamics generated by the previous time-dependent Hamiltonian with the QuTiP library (version 4.4.1) in Python [29]. We consider an idealized two-level qubit (that is, we neglect higher energy level excitations) coupled to a cavity fundamental mode, represented by a Hilbert space truncated to dimension 8 that comprises the vacuum and photon number states up to  $|7\rangle$ .

Given the nature of the dynamical Casimir effect, we expect a monotonic and unbounded parametric generation of photons [30]. Thus, firstly, we ensure that the truncated state-space used in our calculations is large enough to describe the system's dynamics for the analyzed time interval. The Hamiltonian of Eq. (A1) produces one photon per perturbation order (see details in Appendix B), and the vacuum state cannot evolve to a high photon number state directly. We limit the evolution time in the simulations such that the system does not reach the cutoff photon number state  $|7\rangle$  from the initial low-energy states with one-photon transitions. To verify the validity of the Hilbert space truncation, we numerically confirm that the probability of measuring the cavity state  $|7\rangle$  for the given time interval is negligible, as we observe in Figures 5 and 6. The expectation value of the cutoff cavity state,  $\langle \mathbb{I}_{2 \times 2} \otimes |7\rangle \langle 7| \rangle$ , begins acquiring significant values for  $\omega_d = \omega$  and  $\omega > \Omega$ , precisely the parameter regimes expected to produce the DCE.

Secondly, we address the numerical results congruence with the perturbative formulae in the main text. In principle, we numerically compute the dynamics for times exceeding the interval in which perturbation theory is valid. In every simulation, we use a coupling strength of  $g_0 = 0.1\omega$  for time limits of  $wt \approx 200$ , while perturbation theory provides an accurate description of the state for  $gt \approx 1$ , that is, for evolution times differing an order of magnitude  $wt \approx 10$ . We confirm the agreement between the analytic predictions and our numerical results in the regime perturbative regime  $wt < 10$ . Moreover,

we observe the monotonic unbound nature of DCE photon generation beyond the perturbative regime for our ideal model without dissipation. Further notes on decoherence and experimental requirements can be found in Appendix C.

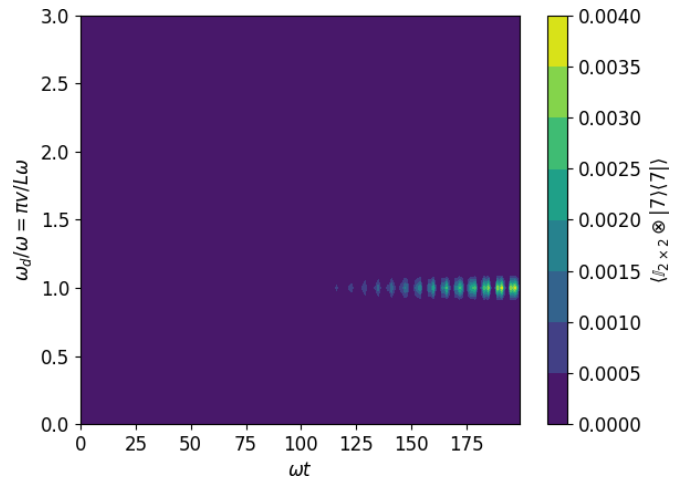


FIG. 5. Expectation value of the projector on the cutoff cavity excited state,  $\mathbb{I}_{2 \times 2} \otimes |7\rangle \langle 7|$ , as a function of time  $t$  in units of the cavity frequency  $\omega$ , for different qubit velocities related to the driving frequency  $\omega_d$ , given as well in units of the cavity frequency  $\omega$ . We consider the same parameter domain as in Figures 2 and 3. The qubit frequency is given by  $\Omega = \omega$ , and the coupling intensity is  $g_0 = 0.1\omega$ . The qubit moves back and forth within the cavity, with constant velocity  $v = L/\pi\omega_d$  in one direction, and  $-v$  after bouncing in the opposite direction.

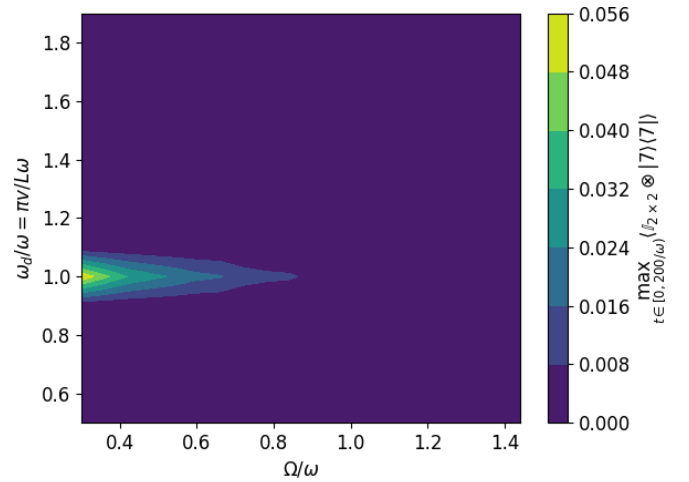


FIG. 6. Maximum value over the time period  $0 < t < 200/\omega$  of the cutoff cavity excited state expectation value, that is  $\max_{t \in [0, 200/\omega]} \langle \mathbb{I}_{2 \times 2} \otimes |7\rangle \langle 7| \rangle$ , as a function of the qubit and driving frequencies,  $\Omega$  and  $\omega_d$  respectively, both in units of the cavity frequency  $\omega$ . We consider the same parameter domain as in Figure 4, and a coupling strength  $g_0 = 0.1\omega$ . The qubit moves back and forth within the cavity at a constant speed  $|v| = L/\pi\omega_d$ .

## Appendix B: Complete and higher order perturbative corrections

In the main text, we characterize the radiation and conditions under which the dynamical Casimir effect takes place by means of typical time-dependent perturbation theory. However, given the extension of the second-order corrections in the coupling's magnitude  $g_0$ , we only considered those terms that become relevant to the DCE. In the following we prove that no other terms produce

noticeable dynamics, even those of third order, by giving the full expressions of the corrections in the series expansion of Eq. (4) in the main text up to third order, for a system described by the Hamiltonian of Eq. (1). We consider the case of resonant qubit and mode frequencies  $\omega = \Omega$ , and the qubit moving back and forth in the cavity with a speed  $|v| = \omega L/\pi$ , which leads to a DCE resonant driving  $\omega_d = \omega$ . Explicitly, the perturbative terms of Eq. (4) are given by

$$g_0\psi^{(1)}(t) = \left( -\frac{2g_0}{3\omega} + \frac{g_0e^{3i\omega t}}{6\omega} + \frac{g_0e^{i\omega t}}{2\omega} \right) |1_2\rangle \otimes |1\rangle$$

$$\begin{aligned} \frac{g_0^2}{2}\psi^{(2)}(t) = & \left( -\frac{13g_0^2}{72\omega^2} - \frac{g_0^2e^{-2i\omega t}}{16\omega^2} + \frac{g_0^2e^{2i\omega t}}{48\omega^2} + \frac{g_0^2e^{-3i\omega t}}{18\omega^2} + \frac{g_0^2e^{-i\omega t}}{6\omega^2} + \frac{ig_0^2t}{6\omega} \right) |0_2\rangle \otimes |0\rangle \\ & + \left( -\frac{\sqrt{2}g_0^2e^{i\omega t}}{6\omega^2} - \frac{3\sqrt{2}g_0^2}{32\omega^2} + \frac{\sqrt{2}g_0^2e^{4i\omega t}}{96\omega^2} + \frac{\sqrt{2}g_0^2e^{2i\omega t}}{12\omega^2} + \frac{\sqrt{2}g_0^2e^{-i\omega t}}{6\omega^2} + \frac{\sqrt{2}ig_0^2t}{8\omega} \right) |0_2\rangle \otimes |2\rangle \end{aligned}$$

$$\begin{aligned} \frac{g_0^3}{6}\psi^{(3)}(t) = & \left( -\frac{7\sqrt{6}g_0^3e^{i\omega t}}{192\omega^3} - \frac{\sqrt{6}g_0^3e^{4i\omega t}}{144\omega^3} - \frac{5\sqrt{6}g_0^3e^{3i\omega t}}{1728\omega^3} + \frac{\sqrt{6}g_0^3e^{7i\omega t}}{4032\omega^3} + \frac{\sqrt{6}g_0^3e^{5i\omega t}}{320\omega^3} + \right. \\ & \left. \frac{649\sqrt{6}g_0^3}{15120\omega^3} + \frac{\sqrt{6}ig_0^3te^{3i\omega t}}{144\omega^2} + \frac{\sqrt{6}ig_0^3te^{i\omega t}}{48\omega^2} + \frac{\sqrt{6}ig_0^3t}{36\omega^2} \right) |1_2\rangle \otimes |3\rangle \\ & + \left( -\frac{49g_0^3e^{i\omega t}}{432\omega^3} - \frac{7g_0^3e^{-2i\omega t}}{216\omega^3} - \frac{g_0^3e^{2i\omega t}}{72\omega^3} - \frac{g_0^3e^{3i\omega t}}{648\omega^3} + \frac{g_0^3e^{5i\omega t}}{720\omega^3} \right. \\ & \left. + \frac{259g_0^3}{1620\omega^3} - \frac{ig_0^3te^{-i\omega t}}{24\omega^2} + \frac{ig_0^3te^{3i\omega t}}{108\omega^2} + \frac{ig_0^3t}{27\omega^2} + \frac{5ig_0^3te^{i\omega t}}{72\omega^2} \right) |1_2\rangle \otimes |1\rangle, \end{aligned}$$

where  $|0_2\rangle$  and  $|1_2\rangle$  are the qubits ground and excited state and  $|n\rangle$  is a photon number state with  $n$  photons. Notice that the only other resonance we have not discussed happens at second order in the ground state component  $|0_2\rangle \otimes |0\rangle$ , which only further proves our point that the relevant dynamics comprise the ground state (which is also the initial state) and states with no qubit excitations and an even number of photons.

## Appendix C: Experimental requirements

A detailed experimental proposal for the realization of the DCE lies beyond the scope of this manuscript. Nevertheless, we will briefly discuss experimental parameter regimes for which an implementation of the microscopic DCE model studied in the main text may be possible. We require a tunable coupling between the qubit and the cavity of magnitude  $g_0 = 0.1\omega$ , that is, only one order of magnitude less than the photon frequency. Moreover,

we assume that the coupling can be modulated in time with a frequency  $\omega_d$  comparable to the cavity frequency  $\omega$ . We analyze the parameter regimes achievable with microwave-frequency superconducting circuits. Within this technology, we consider two candidates.

Firstly, we propose a modified superconducting qubit coupled to a microwave cavity. If the photons have a typical frequency of, for example,  $\omega = 5$  GHz then in order to produce the microscopic DCE one would have to design a qubit with frequency preferably lower, to continue with the example we propose  $\Omega = 2$  GHz, and coupling intensity  $g_0 = 500$  MHz [25]. Then, the system would have to evolve for 40 ns, a short enough time to make dissipation irrelevant since photon lifetimes are typically in the hundreds of nanoseconds [13]. On the other hand, if the coupling intensity is lower, for example  $g_0 = 50$  MHz, the time required to produce photons increases by one order of magnitude, making dissipation relevant. That will be the case for our second experimental proposal, and so we will discuss the effects of dissipation then. For now

we discuss that the qubit will not actually move in the cavity, instead it will *simulate* its movement. As Eq. (1) shows, the only effect movement has on the Hamiltonian is changing the value of the coupling in time. Thus one could argue that as long as an experiment manages to produce that same Hamiltonian, the same phenomena will take place, even if the qubit is static. In the latter case, the qubit could produce the time-dependent coupling if its dipolar moment could change over time. This is due to the fact that the qubit-field interaction Hamiltonian comes from

$$H_{\text{int}} = \hat{\mathbf{d}} \cdot \hat{\mathbf{E}}(x_{\text{qubit}}(t), t) \propto (\sigma^+ + \sigma^-)(a^\dagger + a),$$

where  $\hat{\mathbf{d}}$  is the qubit's dipolar moment operator and  $\hat{\mathbf{E}}(x, t)$  is the electric field amplitude operator throughout the cavity. If the qubit is actually moving, its coupling will change due to the different field amplitudes it will find during its trajectory. However, if the qubit is static but it can change its dipolar moment

$$H_{\text{int}} = \hat{\mathbf{d}}(t) \cdot \hat{\mathbf{E}}(x_0, t)$$

the same Hamiltonian can be produced with an appropriate  $\hat{\mathbf{d}}(t)$ . Proposals and experiments with such qubits already exist [25] which prove their effectiveness and feasibility of the experimental parameters mentioned before.

However, a few caveats may make challenging this experiment. We have been able to pinpoint four of them, namely:

1. Modulating coupling with no qubit frequency modulation.
2. Modulating longitudinal coupling with no transversal coupling.
3. Populating other cavity modes.
4. Populating the third or higher levels on the physical system that models the qubit.

The first two points are related, so we discuss them jointly. The most common way of introducing externally controlled parameters in the system is by means of superconducting interference devices (SQUIDs), which behave as nonlinear inductors that can be tuned with the external magnetic flux that passes through them. However, in our case the circuit must be designed with care that those external parameters will modify only the dipolar moment and not the two lowest levels energy gap defining the qubit (first point). Moreover, the interaction Hamiltonian must be designed to forbid transitions between global states with the same qubit substate. If the latter condition is not met, a different two-level interaction Hamiltonian should be taken into account (second point), as we explain in the following. Suppose that the circuit is described by a static Hamiltonian  $H_{\text{circuit}}$  plus an interaction part of the form  $H_{\text{int}} = \eta O(a^\dagger + a)$ . Both operators  $H_{\text{circuit}}$  and  $O$  act on the degrees of freedom of the circuit, and  $a$  and  $a^\dagger$  act on the cavity mode

state. The circuit-mode coupling  $\eta$  is proportional to  $g_0$ . When the circuit is operated as a qubit the state has to belong to the span of the two lowest eigenvectors  $H_{\text{circuit}}|g\rangle = 0$  and  $H_{\text{circuit}}|e\rangle = \Omega|e\rangle$ . Then one can consider a new, reduced, two-level interaction Hamiltonian  $H_{\text{int},2 \times 2}$  given by the matrix elements  $\langle g|H_{\text{int}}|g\rangle$ ,  $\langle e|H_{\text{int}}|e\rangle$  and  $\langle g|H_{\text{int}}|e\rangle$ , which will produce the same dynamics as long as the circuit is operated as a qubit. By expanding the reduced interaction Hamiltonian in the Pauli basis one has

$$H_{\text{int},2 \times 2} = \eta(|\langle g|O|e\rangle|\sigma_x + |\langle e|O|e\rangle|\sigma_z)(a^\dagger + a),$$

where the energies have been rescaled so that  $|\langle g|O|g\rangle|\sigma_z$  does not appear and the Pauli basis has been rotated to conveniently remove  $\sigma_y$ . Then, the time dependence of the coupling comes from the time dependence of the eigenvectors  $|g\rangle, |e\rangle$ . In addition, it is now clear why the interaction must be engineered so that no transitions between global states with the same qubit substate are allowed. If that were not the case,  $\langle e|O|e\rangle$  would not be zero and a new *longitudinal* coupling would appear with operator  $\sigma_z(a^\dagger + a)$ .

For example, the tunable coupling transmon designed in [25] addresses satisfactorily the first point, that is, it can change the coupling intensity keeping static the qubit's frequency, but not the second. In other words, an experiment using said transmon would have to take into account a longitudinal coupling  $g_z(t)\sigma_z(a^\dagger + a)$ . However, it stands to reason that said transmon is a step in the right direction, and that simple modifications to its design could eliminate that piece in the Hamiltonian. As we have seen, the parameter space of the qubit comprises three parameters, frequency  $\Omega$ , transversal coupling  $g_x$  and longitudinal  $g_z$ . Transmon [25] takes as external parameters only two magnetic fluxes, and so it can only explore a two-dimensional manifold of its three-dimensional parameter space. Thus we conclude that a similar circuit with three SQUIDs could, in principle, independently tune every parameter.

The third point, populating other cavity modes is not a relevant issue for the microscopic DCE but it certainly is for the cavity-enhanced Unruh effect. If the mode structure is composed of equidistant modes, as it should be due to perfectly conducting static boundary conditions imposed in the main text, then producing the microscopic DCE for the fundamental mode would require a driving of  $\omega_d = \omega_0$ , where  $\omega_0$  is the frequency of the fundamental mode, which we called just  $\omega$  in the main text for simplicity. Then the higher modes have frequencies  $\omega_n = (n+1)\omega = (n+1)\omega_d$  which do not resonate with the driving. However, producing the cavity-enhanced Unruh effect in the fundamental mode would require a driving  $\omega_d = \omega_0 + \Omega$ , with  $\Omega$  the frequency of the qubit. If in addition to this  $\Omega \approx \omega_0$ , then that same driving would produce the DCE on the next mode if frequency  $\omega_1 = 2\omega \approx \Omega + \omega = \omega_d$  and both phenomena would combine in a non-trivial way. This problem can be addressed by detuning the qubit or designing the cavity so

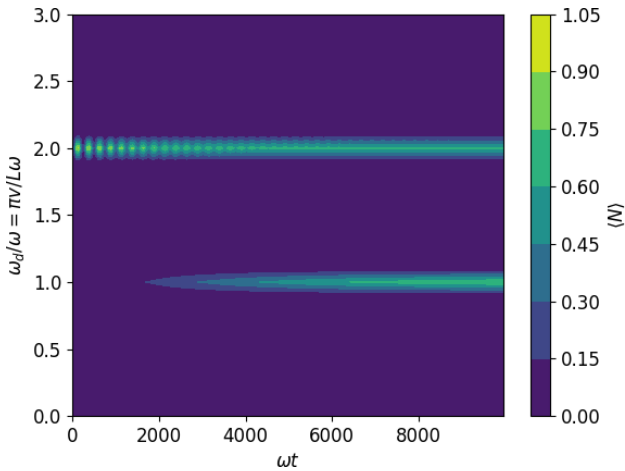


FIG. 7. Number of photons  $\langle N \rangle$  as a function of both time  $t$  in units of the mode's frequency  $\omega$  and driving frequency  $\omega_d$  in units of the same mode's frequency  $\omega$ . The qubit frequency is given by  $\Omega = \omega$ , and the coupling intensity is  $g_0 = 0.025\omega$ , to mimic the parameter regime that the experimental proposal with an actual mechanical oscillation would impose on the system. The driving frequency was produced by a qubit moving back and forth within the cavity, with constant velocity  $v = L/\pi\omega_d$  in one direction, and  $-v$  after bouncing in the opposite direction. The collapse operators considered in the Lindblad master equation were  $0.025\omega a$  and  $0.025\omega\sigma^-$ .

that its modes have not a harmonic structure by means of SQUIDS that add inductance to the boundary conditions.

The last caveat of the first experiment we propose is populating higher levels of the qubit system. If the qubit's complete level structure is nearly harmonic the DCE will be combined with a new resonance at second order, in which two photons and two qubit excitations take place in a magnitude comparable to the DCE. We conclude the qubit's complete level structure must be anharmonic, at least with regard to the third level, or said level will have to be taken into account.

The second experiment we consider makes use of a film bulk acoustic resonator (FBAR) in order to relate the modulation of the coupling to an actual moving piece in the system. Some recent literature has considered this experiment with small variations before, see Wang *et al.*[26]. The idea is to couple the qubit and the cavity by means of a capacitor composed of two conducting strips and dielectric material between them. Those strips and dielectric material form the FBAR, which can be cooled down to its ground mechanical level as was proven in [27]. The reported frequency of its fundamental mechanical mode is around 6 GHz. Then the FBAR would be driven by means of a piezoelectric material with its fundamental frequency so that  $\omega_d = 6$  GHz. Note that the value of  $\omega_d$  falls right into the microwave regime, and so cavity modes and qubit frequencies  $\omega$  and  $\Omega$  can be engineered in the context of microwave superconducting circuits to match it. The coupling intensity  $g_0$  is con-

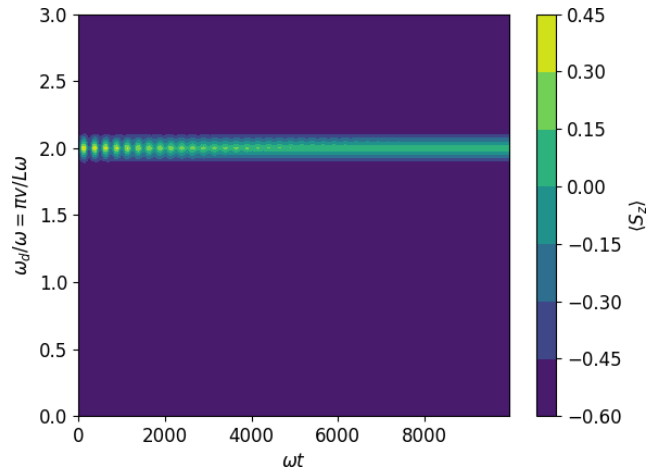


FIG. 8. Qubit excitation  $\langle S_z \rangle$  as a function of both time  $t$  in units of the mode's frequency  $\omega$  and driving frequency  $\omega_d$  in units of the same mode's frequency  $\omega$ . The qubit frequency is given by  $\Omega = \omega$ , and the coupling intensity is  $g_0 = 0.025\omega$ , to mimic the parameter regime that the experimental proposal with an actual mechanical oscillation would impose on the system. The driving frequency was produced by a qubit moving back and forth within the cavity, with constant velocity  $v = L/\pi\omega_d$  in one direction, and  $-v$  after bouncing in the opposite direction. The collapse operators considered in the Lindblad master equation were  $0.025\omega a$  and  $0.025\omega\sigma^-$ .

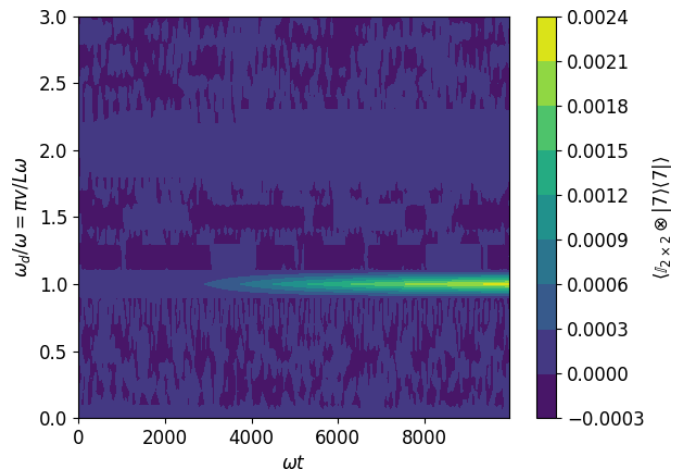


FIG. 9. Expectation value of  $\mathbb{I}_{2 \times 2} \otimes |7\rangle\langle 7|$  as a function of both time  $t$  in units of the mode's frequency  $\omega$  and driving frequency  $\omega_d$  in units of the same mode's frequency  $\omega$ . The qubit frequency is given by  $\Omega = \omega$ , and the coupling intensity is  $g_0 = 0.025\omega$ , to mimic the parameter regime that the experimental proposal with an actual mechanical oscillation would impose on the system. The driving frequency was produced by a qubit moving back and forth within the cavity, with constant velocity  $v = L/\pi\omega_d$  in one direction, and  $-v$  after bouncing in the opposite direction. The collapse operator considered in the Lindblad master equation were  $0.025\omega a$  and  $0.025\omega\sigma^-$ .

nected to the lengths of the parallel strips of the FBAR by a no trivial integral formula [26], but typical values of tens of  $\mu\text{m}$  lead to couplings of  $g_0 = 0.01\text{--}0.05\omega$ , an order of magnitude weaker than the one used in the main text. Then one must consider the evolution of the system for longer times in order to produce a measurable amount of photons. In that case, decoherence will have time to become relevant and reduce the number of photons, which raises the question of whether the DCE will be observable or not. Figures (7 - 9) show that the DCE photon production could be observed for the same simplified

system of previous simulations evolving under a Lindbladian composed of Hamiltonian in Eq. (1) with resonant mode's, qubit's and driving frequencies  $\omega = \Omega = \omega_d$  with weak coupling  $g_0 = 0.025\omega$  plus the collapse operators  $0.025\omega a$  and  $0.025\omega \sigma^-$ , with  $a$  the photon annihilation operator and  $\sigma^-$  the qubit relaxation operator. Notice that a dissipation as intense as the coupling puts the system in a parameter regime between the strong and weak coupling regime. Since 2004 [13] it is possible and typical in this quantum technology to build and use superconducting circuits in the strong coupling regime, so the dissipation considered here is an overestimation.

---

[1] G. T. Moore, *Journal of Mathematical Physics* **11**, 2679 (1970).

[2] B. S. DeWitt, *Physics Reports* **19**, 295 (1975).

[3] S. A. Fulling and P. C. W. Davies, *Proceedings of the Royal Society A: Mathematical, Physical and Engineering Sciences* **348**, 393 (1976).

[4] P. C. W. Davies and S. A. Fulling, *Proceedings of the Royal Society of London. A. Mathematical and Physical Sciences* **356**, 237 (1977).

[5] E. Yablonovitch, *Physical Review Letters* **62**, 1742 (1989).

[6] W. E. Lamb and R. C. Retherford, *Phys. Rev.* **72**, 241 (1947).

[7] H. B. G. Casimir and D. Polder, *Phys. Rev.* **73**, 360 (1948).

[8] H. B. G. Casimir, *Proceedings of the Koninklijke Nederlandse Akademie van Wetenschappen* (1948).

[9] S. A. Fulling, *Physical Review D* **7**, 2850 (1973).

[10] P. C. W. Davies, *Journal of Physics A: Mathematical and General* **8**, 609 (1975).

[11] W. G. Unruh, *Physical Review D* **14**, 870 (1976).

[12] S. Hawking, *Nature* **248**, 30 (1974).

[13] A. Wallraff, D. I. Schuster, A. Blais, L. Frunzio, R.- S. Huang, J. Majer, S. Kumar, S. M. Girvin, and R. J. Schoelkopf, *Nature* **431**, 162 (2004).

[14] C. M. Wilson, G. Johansson, A. Pourkabirian, M. Simoen, J. R. Johansson, T. Duty, F. Nori, and P. Delsing, *Nature* **479**, 376 (2011).

[15] P. Lähteenmäki, G. S. Paraoanu, J. Hassel, and P. J. Hakonen, *Proceedings of the National Academy of Sciences* **110**, 4234 (2013).

[16] R. de Melo e Souza, F. Impens, and P. A. M. Neto, *Physical Review A* **97**, 032514 (2018).

[17] J. M. B. Kellogg, I. I. Rabi, and J. R. Zacharias, *Nature* **137**, 658 (1936).

[18] D. Braak, *Physical Review Letters* **107**, 100401 (2011).

[19] E. T. Jaynes and F. W. Cummings, *Proceedings of the IEEE* **51**, 89 (1963).

[20] S. Felicetti, C. Sabín, I. Fuentes, L. Lamata, G. Romero, and E. Solano, *Physical Review B* **92**, 064501 (2015).

[21] M. O. Scully, V. V. Kocharovsky, A. Belyanin, E. Fry, and F. Capasso, *Physical Review Letters* **91**, 243004 (2003).

[22] B. L. Hu and A. Roura, *Phys. Rev. Lett.* **93**, 129301 (2004).

[23] M. O. Scully, V. V. Kocharovsky, A. Belyanin, E. Fry, and F. Capasso, *Phys. Rev. Lett.* **93**, 129302 (2004).

[24] A. Belyanin, V. V. Kocharovsky, F. Capasso, E. Fry, M. S. Zubairy, and M. O. Scully, *Phys. Rev. A* **74**, 023807 (2006).

[25] S. J. Srinivasan, A. J. Hoffman, J. M. Gambetta, and A. A. Houck, *Physical Review Letters* **106**, 083601 (2011).

[26] H. Wang, M. P. Blencowe, C. M. Wilson, and A. J. Rimberg, *Physical Review A* **99**, 053833 (2019).

[27] A. D. O'Connell, M. Hofheinz, M. Ansmann, R. C. Bialczak, M. Lenander, E. Lucero, M. Neeley, D. Sank, H. Wang, M. Weides, J. Wenner, J. M. Martinis, and A. N. Cleland, *Nature* **464**, 697 (2010).

[28] M. P. Blencowe and H. Wang, *Philosophical Transactions of the Royal Society A: Mathematical, Physical and Engineering Sciences* **378**, 20190224 (2020).

[29] J. Johansson, P. Nation, and F. Nori, *Computer Physics Communications* **184**, 1234 (2013).

[30] M. Uhlmann, G. Plunien, R. Schützhold, and G. Soff, *Physical Review Letters* **93** (2004), 10.1103/physrevlett.93.193601.